Applied GIS

ISSN: 1832-5505
Vol-9 Issue-04 Oct 2021

Performance of Fuzzy Logic Controller and Unified PowerFlow Controller Using a Power Electronics Integrated Transformer

M MOUNIKA

ASSISTANT PROFESSOR

mouni3771@gmail.com

G VAMSI KRISHNA

ASSISTANT PROFESSOR

kvamsi706@gmail.com

C SUMALATHA

ASSISTANT PROFESSOR

sumalathacherukuri@gmail.com

DEPT OF ELECTRICALAND ELECTRONICS ENGINEERING, Sri Venkateswara Institute of Technology,N.H 44,Hampapuram, Rapthadu, Anantapuramu, Andhra Pradesh 515722

Abstract:

The Custom Power Active Transformer (CPAT) is a power device linked transformer that provides various forms of assistance to the cross zone via its helper windings. In this work, we describe a Unified Power Flow Controller (UPFC) that makes use of this transformer. The CPAT design incorporates a shunt-strategy mixing transformer with three individual stages. This cable connects to a substation and can only handle the current and voltage at a transformer's terminals via separate force gear converters. The capacity of the CPAT to provide UPFC administrations, such as responsive force pay, voltage guideline, noise disposal, and power stream management, is investigated in this work. Its utility as a between-transport coupling transformer providing the required matrix administrations is shown by a CPAT-UPFC recreation with a solid network and a 5-transport power framework. To further validate its transient and consistent state response, we also look at how the CPAT-UPFC affects the force framework under load problems. In addition, the three-stage CPAT-UPFC's activity is revealed by a test model, confirming that it consistently operates according to the hypothetical demands.

IndexTerms--
Powertransformers,Magneticcircuits,Powercontrol,Powertransmission,fuzzylogiccontroller.

INTRODUCTION

Some challenges and specialised complications have arisen as a result of the increased interest in conveying age in an effort to inspire phenomenal network commitments. Due to the unpredictable behaviour of the sustainable age and the increasing demand for electrical power, there have been several advancements in the design and operation of substations to solve these problems [1]. The force architecture has evolved to respond to such demands with a combination of monitoring and control features, ensuring a robust, practical, and smart electric system [2]. Force device converters, which have shown some beneficial benefits on the

ISSN: 1832-5505
Vol-9 Issue-04 Oct 2021

appropriation arrange [3-5] and transmission arranges [6-8], have authorised these features. The adaptability, consistency, and reliability of transmission and distribution frameworks may be enhanced with the use of FACTS, which have shown themselves capable of providing many forms of support [9]. The UPFC is considered the most versatile device among these devices for reducing line congestion and increasing the capacity of existing lines. Large detachment transformers, complicated staggered topologies, or sequential converters have all been used to connect intensity hardware converters in order to provide UPFC services.

attention to the line power that was investigated [10-12]. As a result of the requirement to eliminate massive detachment transformers, transformer-less thinking solutions, such as stunned topologies, have emerged. Regardless, such topologies manage the whole evaluated line voltage, which always necessitates a perplexing architecture. An attractive solution is to employ transformers, which provide isolation, to connect shunt and plan power electronic devices to the force framework. However, while thinking about high force pay frameworks, size, cost, and perception are additional concerns. In response to these issues, there has been continuous discussion about employing off-the-shelf converters or creating a force hardware based transformer as a means to reconcile intensity electronic devices in a standard transformer. However, these approaches have either focused on a single kind of compensation [12], using explicit applications, or necessitating sophisticated designs and high levels of force. The newly-introduced CPAT demonstrates a centrally-structured solid-state transformer that links distribution transformers to arrangement and shunt power hardware converters. The Sen Transformer and a CPAT are functionally identical since they combine many transformers into one. The proximity of intensity device converters in a CPAT, as opposed to the progression response in a Sen Transformer, is the primary reason why the CPAT offers a few advantages over the Sen Transformer. Receptive force compensation, noises end, and inrush current alleviation are only a few of the shunt administrations made possible by the CPAT. Not all of these services are available from Sen Transformers. Research on the CPAT has focused on single-stage applications and composition distribution as a UPQC (Unified Power Quality Conditioner). Theoretically, a CPAT's output windings may be used for any shunt-game plan application, which opens up gearbox applications as well.
In order to resolve the confinement requirement, many published methods use either transformer-less approaches or methods relying on force devices as transformers. Although similar configurations have been employed in certain applications, eliminating the need for bulky line transformers for segregation, the complex force hardware layout provides a challenge. Because of its essential role in coordinating voltage levels across different

ISSN: 1832-5505
Vol-9 Issue-04 Oct 2021

transports, CPAT force transformers contain both arrangement and shunt transformers. In this case, an isolated UPFC

replacing any force transformer with a CPAT allows for the introduction of using fragmented force converters. Thus, this allows for the incorporation of a UPFC into any force transformer. In order to regulate the flow of power between the mandatory and elective windings, provide responsive force compensation, and dispose of noise, this study suggests the CPAT-UPFC, which makes use of three single-stage CPATs. For power stream control applications, the three-stage CPAT plan is given, shown, and disengaged, depending on the clarity of its connection with the circuit. Power stream management between two in-number frameworks has been the focus of the CPAT-UPFC's redirections and assessments. For the purpose of controlling power streams and operating under load irritations in the force framework, the CPAT-UPFC has also been modelled as a substation transformer in a 5-transport power framework. Lastly, the observed steady proliferations and exploratory results reveal that a CPAT-UPFC is unable to provide satisfactory assistance of this kind. The work is organised as follows: Section II presents the models and theories behind a three-phase CPAT, which is considered to be an action-speculative approach. Thirdly, we suggest a three-phase CPAT controller for UPFC use. The CPAT-UPFC is evaluated for redirection under the conditions of a solid framework relationship in Part IV. District V is now conducting a replication of the CPAT-UPFC on a test stage and in its role as a substation transformer in the a5 - transport power framework. Finally, in Section VI, we wrap up.

I. THEORYOFOPERATION

A. Configuration

A single-stage CPAT that integrates a transformer's layout and shunt windings has been developed and launched. The CPAT's activity rule is predicated on the assumptions that shunt electric circuits are proportional to windings twisted over equal appendages and arrangement electric circuits are proportional to windings twisted over regular appendages. The three-stage $\mathbf{O}PAT$ in the transmission application is shown in Fig.1 when these criteria are taken into account. A three-phase dynamic converter is included in the plan, which consists of three single-stage CPATs. The name of each CPAT is $\mathbf{O}PATp$, and p monitors the stage number. In each CPAT, akk and ipk take care of the winding voltages and floods, with k keeping an eye on the winding number. Similar to a standard transformer, the system is connected to the essential and associate windings of a $\mathbf{O}PAT$ (k=1, k=4). Connected to the shunt and procedure windings, a three-phase dynamic converter regulates the current in the shunt winding and the voltage in the strategy winding (k=2, k=3). In addition to directing the DC transport voltage, the shunt converter provides various forms of help to the vital twisting, such as consonant disposal and responsive force pay. In order to function as a UPFC, the arrangement converter manages the

ISSN: 1832-5505
Vol-9 Issue-04 Oct 2021

receptive and dynamic forces using the optional twisting.

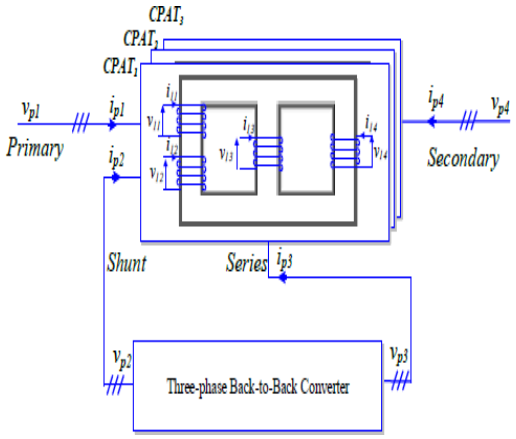

Fig.1.Three-phaseCPATconfigurationusingthree single-phase CPATs and a back-to-backconverter.

B. Modeling

1. NON-LINEAR TRANSFORMERMODEL

A similar model (Fig. 2 (a)) may be constructed by discretizing the attractive development courses in (Fig. 2). K=1 (fundamental), 2 (shunt), 3 (plan), and 4 (optional) are the bending types shown in Fig. 2(a), and m is the number of people. This circuit's developments are shown as centre linkage fluxes (φcm), winding fluxes (φk), spillage developments per winding (Lk), and centre spillage flux ($\varphi 0$). The non-straight reluctances RY and RL communicate with the centre appendages and loads, and the value is dictated by the B-H features of the centre material. Figure 2(b) shows a non-straight reluctance as a controlled magneto-perspective source in a closed hover between input movement and yield magneto-goal power (F). The appendage or load length (l), zone (An), and centre B-H attributes shown in Fig. 3 would determine the limiting magneto-rationale power that this model would convey. Direct reluctances are used to address winding spillage reluctances (Sk) and centre spillage hesitance (R0). To measure spill resistances, the transition path length, mean zone, and relative air viscosity (μ0=4π10-7). The progress of each winding is linked to a winding electric circuit, as shown in Figure 2(c), in order to illustrate winding issues and pinpoint proportional catastrophes. winding impediment (Rk), relative focus distress check (Rc), and unexpected winding current (iek) may affect the same transformer winding current (ik) for any applied winding voltage (ak). The sensible

As shown in Figure 2(c), the current is determined by the appropriate magneto-procedure for the winding's deduction power (Fk) and the number of turns (Nk). The persuasive voltage (aek) in the winding electric circuit is what makes the connected circuit's turning proceed.

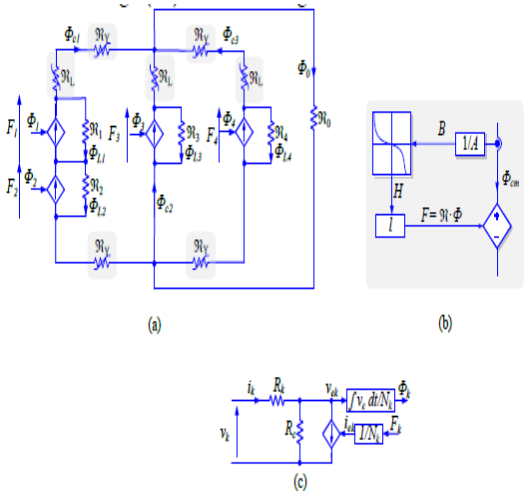

Fig. 2. Equivalent magnetic circuit model of asingle-phase CPAT. (a) core equivalent magneticcircuit,(b)non-linearcorereluctancemodel,and (c)windingequivalentelectriccircuit.

2. LINEARTRANSFORMERMODEL

A direct representation of the model may be obtained by converting the attractive circuit (Fig. 2) into its corresponding electric circuit (Fig. 3). Ideal couplings between the necessary, shunt, arrangement, and optional windings are assumed to be maintained via non-direct centre impedances, which are large and constant. $Le1$, $Le2\ and Le3$ and $Re1$, $Re2\ and Re3$ each address the centre charging impedances and centre disaster safeguards separately. The zero-course-of-action charging inductances and transformer leakage inductances are handled separately by $\boldsymbol{Xk}$ and L0. Next to two windings on the inside and

ISSN: 1832-5505
Vol-9 Issue-04 Oct 2021

aid at the furthest places, the proportional circuit (Fig. 3) is fuzzy from the circuit of a three-stage transformer. The normal method of testing transformers for low-and mid-rehash transient multiplications may settle the circuit's constraints.

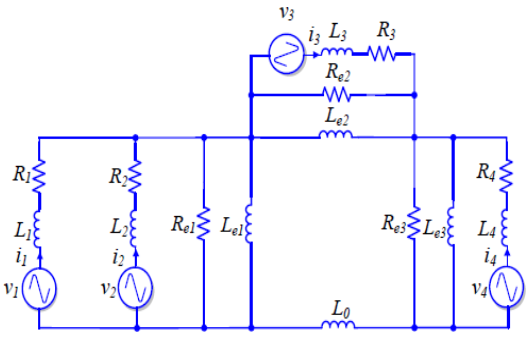

Fig. 3. Equivalent linear electric circuit of a single-phaseCPAT.

3. POWERCONVERTERSMODEL

The architecture shown in Figure 4 was used to conduct the sequence of action in Figure 1. The CPAT's shunt and approach windings were linked to a three-stage sequential converter. The shunt converter, similar to a standard UPFC, solved the issue of sharing repeat music by acting as a current controlled voltage source inverter (CCVSI) equipped with an LCL channel. The basic reduction of trade repeat music and resonance repeat was used to choose the channel parameters L1sh, ash, and L2sh. The shunt damping obstacle (Rsh) was used to develop channel resonation damping. A three-phase four-wire topology was used to connect the converter and ensure that the shunt windings would receive a tridentate consonant current. There could be no doubt about the transportcapacitor(Cdc)andcontrolstheshuntconverter current($ip2sh$).Essentialvoltage($vp1$)andcurrent($ip1$)wereassessedtosynchronizethe charging symphonies that the transformer needed. Thus, the cross area would not be required for the mixing of such harmonious current parts via the shunt winding. With the shunt converter controller, a robust DCtransportvoltage($vdc1$,$vdc2$)overeachDCto provide the basic forms of assistance to $ip1$ and to combine the shunt converter voltage ($ap2$) with vp1. The shunt converter controller's yield PWM indicators controlled the shunt current via the shunt converter's converter switches, as seen by the key reference.

Equipped with an LC channel to disable trading repetition suggestions of the yield voltage ($ap3$), the strategy inverter served as a voltage source inverter. Similar to how the channel limitations $\mathbf{O}sea$ and $\mathbf{O}serandRyea$ were determined by the basic restrictions of resonation dampening and trading repetitive music. In order to regulate the game-plan voltage ($ak3$), the imperative associations accommodated $ik4$ demonstrated the optional voltage ($ak4$) and current ($ik4$). The action inverter achieved the necessary reference approach voltage using the yield pulse width modulation (PWM) signals given by the game-plan converter controller. An regular CPAT centre understood a three-stage CPAT structure, as shown in Fig.4, which associated each season of the basic, shunt, strategy, and assist winding.

Figure 5 shows a shared model of the two converters that is connected to the CPAT's fast model. Using this setup, researchers may examine low-to mid-repeat stray CPAT introductions. As shown in Figure 5, the conventional approach accounts for the impact of trade over music by use of a directly regulated voltage source. Using a three-phase three-wire converter design was necessary since this model does not take music into account. The conscious shunt converter power (P2) and strategy converter power ($P3$) were used to mimic the typical DC transmission at each model second (adc), as shown in (2).

$$V_{dc1}=V_{dc2}=-_2\int -\frac{1}{C_{dc}V_{dc1}}\frac{P_2+P_3}{}dt---(1)$$

Applied GIS

ISSN: 1832-5505
Vol-9 Issue-04 Oct 2021

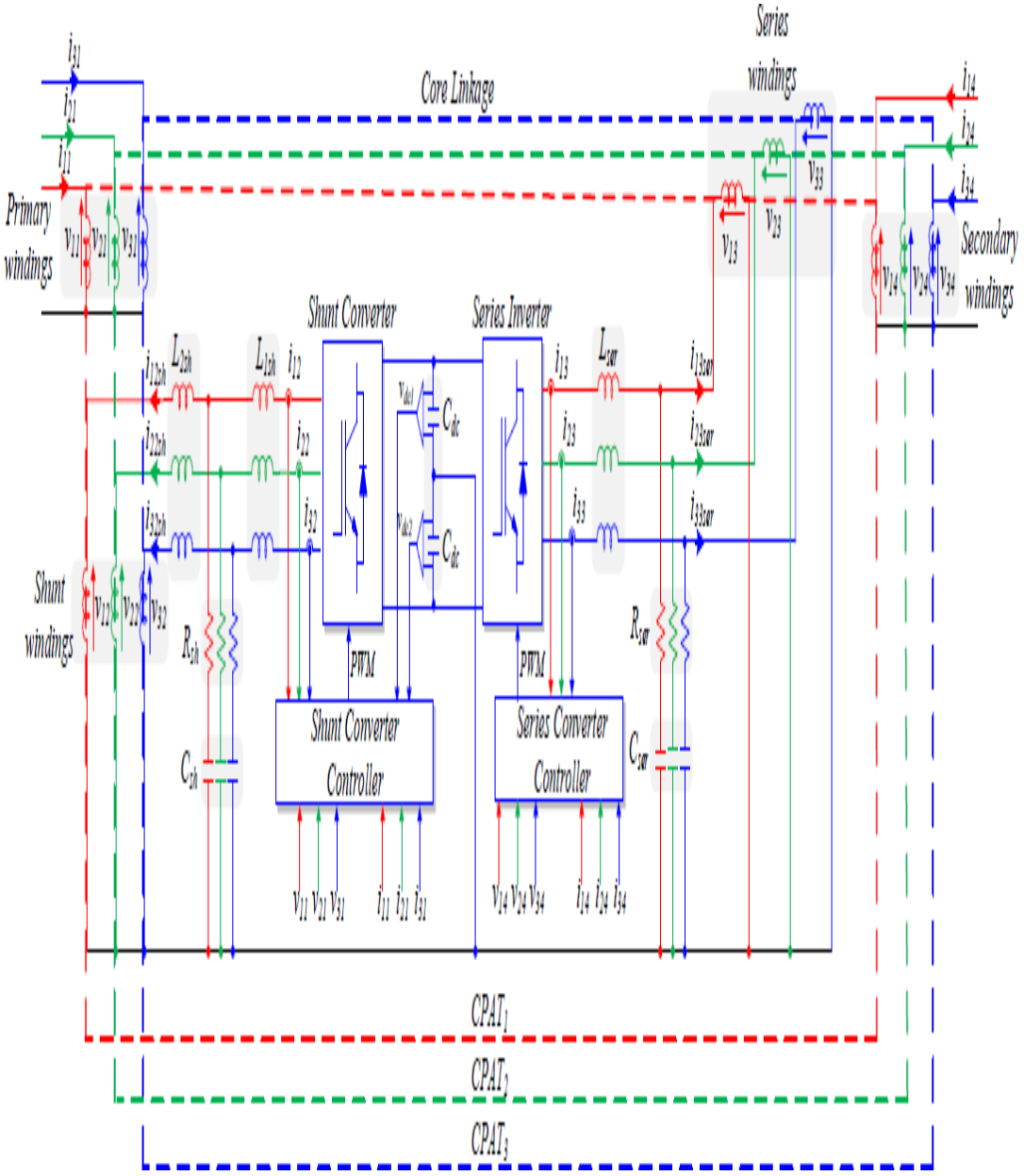

Fig.4.Backtobackconvertertopologyforthethreephase CPAT

Applied GIS

ISSN: 1832-5505
Vol-9 Issue-04 Oct 2021

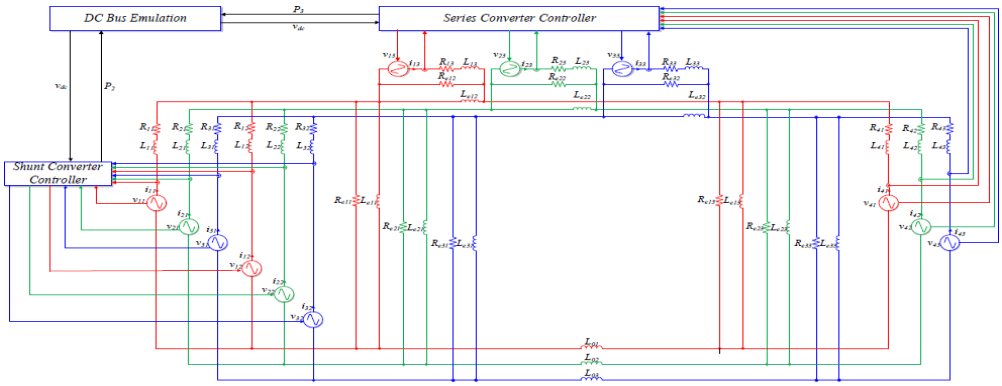

Fig.5.AveragemodelofthethreephasesCPATandbackto backconverter

II. CONTROLOFTHREE-PHASECPAT-UPFC

Two free controllers are shown in Figures 6 and 7, which constitute the CPAT-UPFC control scheme. The goals of the shunt converter controller, as mentioned earlier, as shown in Figure 6, are as follows: to maintain a consistent DC transport voltage relative to the reference DC transport voltage ($Xdc \prod$), to control the receiving force through the essential based on the reference responsive force ($Q1 \prod$), and to eliminate harmonic components in the essential current. Essential framework voltage ($ap1$), essential matrix current ($ip1$), shunt converter current ($ip2$), and DC transport voltages ($adc1\ andadc2$) are the intentional attributes for these goals. While controlling the dynamic and receptive force courses via the optional twisting of the CPAT, the arrangement converter controller shown in Figure 7 simultaneously takes reference of the dynamic ($P4 \prod$) and responsive ($Q4 \prod$) power. A controller that controls a heap transmission voltage ($Vload$) may also set $Q4 \prod$.

Thedeliberatefactorsforthesecontroldestinati onsareauxiliarymatrixvoltage($vp4$),optionallatticecur rent($ip4$)andloadtransportvoltage($vload$).Both$ip2$an darrangement

convertercurrent($ip3$)areadditionallyutilizedfor

over-currentsecurityineveryconverter.

Estimationsfromeveryengineeringwere

looked at using the Sample and Hold to get the n test estimate of every intentional variable. The synchronisation framework utilises the deliberate voltages to select their proportional recurrence (ω), synchronising signals $sin⟦(\omega t)⟧$, $cos⟦(\omega t)⟧$ size (V) and simultaneous reference-outline parts ($v\alpha$, lookingattradingstateofeachswitch(g)toachievethebasi ccontroltargets.

In order to accomplish the massive control goals, the shunt controller that first appeared in Figure 6 has recently been studied in [17] and [18]. The primary reference shunt current ($ik2 \prod$) is used by a Proportional Resonant (PR) controller to determine the shunt converter current. The reference includes a head section ($ik2f \prod$) that controls the DC transport voltage and responsive force via the essential exactly as a sounds section ($ik2h \prod$) that guides the consonant flows in ip1. The major current's important weakening frequencies ($ip1$) are employed by a Resonant Controller to settle symphonic parts injected via the shunt converter. The DC transport voltage is controlled by two Proportional Integral (PI) controllers, one for the typical DC transport voltage (adc) and the other for the relationship between the higher and lower DC voltages ($adc1\ andadc2$). A PI controller selects the basic open current to be embedded via the shunt converter in order to get the essential reference $Q1 \prod$, which is used to compose the responsive force through the central. Using equation (2), we can get the input receptive force ($Q1$).

$$Q_1 = \frac{1}{\sqrt{3}}[V_{11}\ V_{21}\ V_{31}]\begin{bmatrix} 0 & -1 & 1 \\ 1 & 0 & 1 \\ -1 & 1 & 0 \end{bmatrix}\begin{bmatrix} i_{11} \\ [i_{21}] \\ i_{31} \end{bmatrix} \quad (2)$$

$v\beta$).These signals, coupled with the reference and purposeful factors, were sent to the blurry controller, which selected the massive levelling of the converter (M). The PWM module then selected the

ISSN: 1832-5505
Vol-9 Issue-04 Oct 2021

Figure 7 shows the three stages of the arrangement controller: reference receptive force calculation, optional current figuring, and auxiliary current controller. Physical means or an optional voltage controller may be used to adjust the reference receptive force ($Q4$ ∏), which determines the responsive capacity needed to maintain the reference load voltage ($Xload$ ∏).

Based on the reference dynamic and responsive force ($P4$ ∏, $Q4$ ∏) and the fixed reference-outline optional voltage ($a\beta 4$, $a\beta 4$), the auxiliary current estimate determines the same fixed reference-outline optional current ($i\beta 4$, $i\beta 4$). In condition (3), the estimates are summarised [25].

Utilizingthe auxiliarysynchronizingsignals 〖

sin 〖(ωt)〗 〗_4, 〖cos 〖(ωt)〗 〗_4the $i\alpha 4$ and$i\beta 4$arechangedtotheirill-definedthree-phase

wholes($ip4$ ∗).APRcontrollertunedtothedire

repeat ($\omega 4$)controls the associate current ($ip4$)toorchestratethereference$ip4$ ∗.Theresultantreference approach voltage ($vp3$ ∗) is isolated by theDCtransportvoltage(vdc)topicktheequalityarchive ofthecourseofactionconverter (Mp3).

$$[i_{\alpha 4} \quad i_{\beta 4}] = \frac{1}{V_{\alpha 4}{}^2 + V_{\beta 4}{}^2} [P^* \quad Q^*] \begin{bmatrix} V_{\alpha 4} & -V_{\beta 4} \\ V_{\beta 4} & V_{\alpha 4} \end{bmatrix} \quad (3)$$

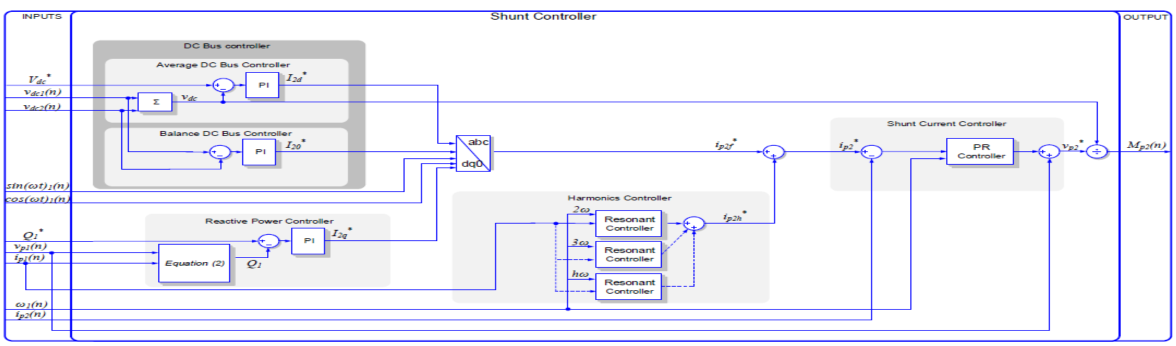
INPUTS
Shunt Controller
OUTPUT
DC Bus controller
Average DC Bus Controller
Balance DC Bus Controller
V_{dc}^*
$v_{dc1}(n)$
$v_{dc2}(n)$
Σ
v_{dc}
PI
I_{2d}^*
PI
I_{20}^*
abc
dq0
$sin(\omega t)_1(n)$
$cos(\omega t)_1(n)$
Reactive Power Controller
Q_1^*
$v_{p1}(n)$
$i_{p1}(n)$
Equation (2)
Q_1
PI
I_{2q}^*
$\omega_1(n)$
$i_{p2}(n)$
Harmonics Controller
2ω
3ω
$h\omega$
Resonant Controller
Resonant Controller
Resonant Controller
i_{p2h}^*
i_{p2f}^*
Shunt Current Controller
i_{p2}^*
PR Controller
v_{p2}^*
$M_{p2}(n)$

Fig.6.shuntcontrollerblockstructure

Applied GIS

ISSN: 1832-5505
Vol-9 Issue-04 Oct 2021

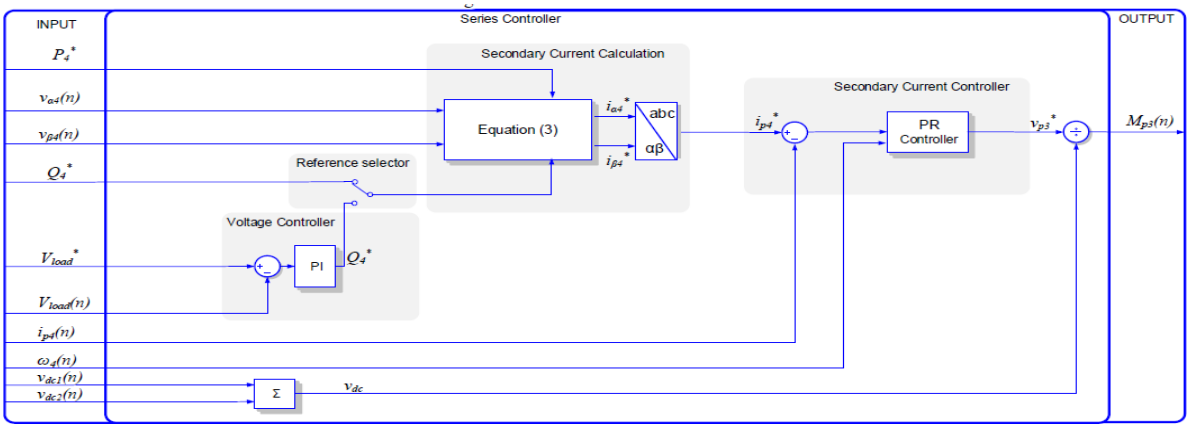

Fig.7.seriescontrollerblockstructure

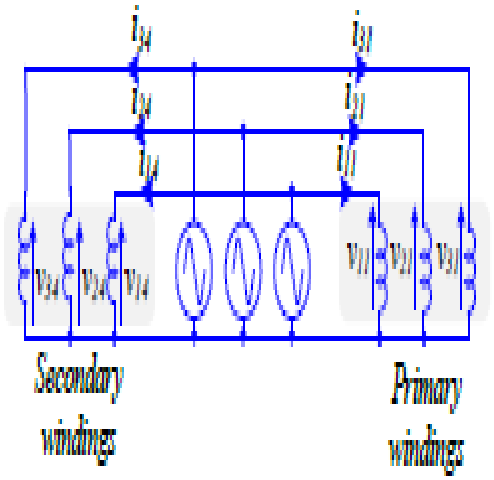

Fig.8.stiffgridconnectiontoprimaryandsecondary windings

III. Fuzzylogiccontroller:

Principles based on the mainstay of fuzzy logic controllers. What matters is the data type and the results. Error value and error value change are two properties of the fuzzy logic controller input. Data values and ruleset configuration determine the yield value. Limits of the variable from -1 to 1. Boolean logic reality check: the variables may be either 0 or 1. We may classify fuzzy logic controllers into three main types: fuzzification, rule networks, and defuzzification. The relationships between the three controllers are shown in the circuit diagram below.

Applied GIS

ISSN: 1832-5505
Vol-9 Issue-04 Oct 2021

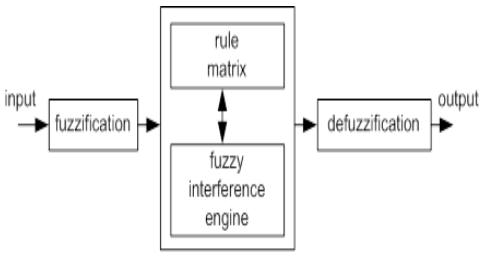

Fig.9.Fuzzylogicanalysisandcontrol

Fluffy principlesareorderedreliesoninformationandyieldparticipationcapacities.Theschematiccircuit chart of participation capacities demonstratedasfollows

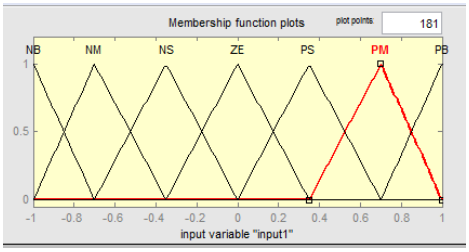

Fig.10.Error

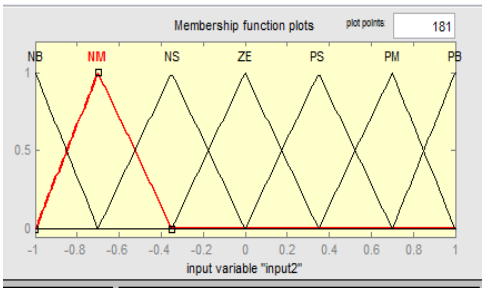

Fig.11.Changeinerror

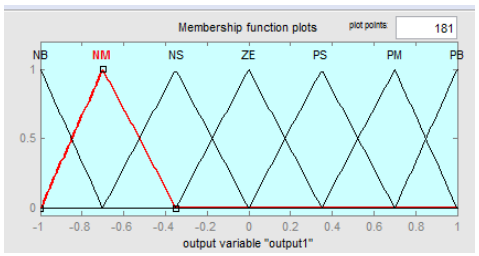

Fig.12.Output

Verror /error	**NB**	**NM**	**NS**	**ZE**	**PS**	**PM**	**PB**
NB	NB	NB	NB	NB	NM	NS	ZE
NM	NB	NB	NB	NM	NS	ZE	PS
NS	NB	NB	NM	NS	ZE	PS	PM
ZE	NB	NM	NS	ZE	PS	PM	PB
PS	NM	NS	ZE	PS	PM	PB	PB
PM	NS	ZE	PS	PM	PB	PB	PB
PB	ZE	PS	PM	PB	PB	PB	PB

Table.1.Fuzzylogiccontrollerrules

Fuzzy logic controllers take error and change-in-error and yield-input estimates into account. Each of the five triangle capabilities is blended into the principles. The data and yield participation capacity fundamental chart was shown in figures 10, 11, and 12. 'Positive little (PS)', 'Zero (Z)', 'negative enormous (NL)', 'negative little (NS)', and 'negative enormous (NL)' are the interfaces between these fluffy sets. The seven components of error and its transformation are guided by 49 fluffy standards (FLC contribution).

IV. Simulationresults:

a. SimulationresultsusingPIcontroller:

The CPAT configuration in Fig. 4 was shown using the exhibiting technique discussed in Section II, subject to the limits imposed in Table I. N is the number of turns, lL is the length of the appendage, lY is the length of the load, and A is the area of the appendage that make up the transformer model.

A standard solid matrix was connected to the primary and secondary windings, as shown in Figure 8. In this setup, the necessary and optional are both powered by the same voltage, therefore there is no flow of force between them. This way, the centre might be energised by isolating the CPAT's polarising current between the two windings. While that was happening, the shunt and arrangement converters each introduced zero current and voltage since the shunt and arrangement controllers were both disabled. The majority of the necessary current was third, fifth, and seventh order request music, as seen in Figure 13. Important CPAT charging current and DC transport guideline current made up the majority of the necessary current in this case since there was no force stream between the two. Figure 14 shows how the crucial current waveform was removed by the shunt music controller set to these frequencies. There was no need to be concerned about uncompensated higher-request noises since these symphonious flows would not be magnified. The vital current would extend beyond the polarising current but remain below the gauges. Because the shunt open force controller was locked in with a reference of 0 VAR, the shunt converter provided the

as seen in Figure 15, the CPAT's necessary response force. With a reference of 5 kW and a power stream of 0 kVAR

ISSN: 1832-5505
Vol-9 Issue-04 Oct 2021

between the essential and optional, the partner current controller was locked in (Fig. 16). The action converter allowed the strategy bending to adjust the equivalent impedance between the basic and discretionary windings in response to the course of action. Because the auxiliary added capacity to the network, which the essential obtained, the driving force also shifted at that moment (Fig.17). As seen in Figure 18, the DC transport controller maintained a constant DC transport voltage throughout the operation. As a consequence of using this reference, the essential and helper current waveforms are shown in Figure 19. That the sounds controller was able to adequately contract the basic current music at the tuned frequencies throughout the movement is shown by the graph.

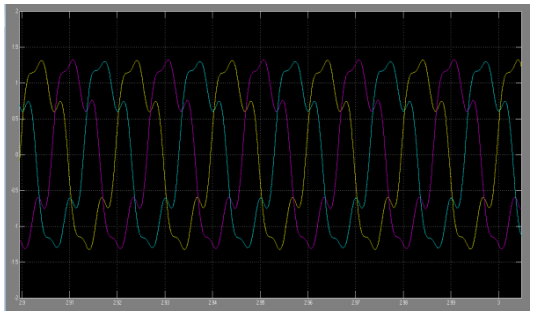

a. Ipabc

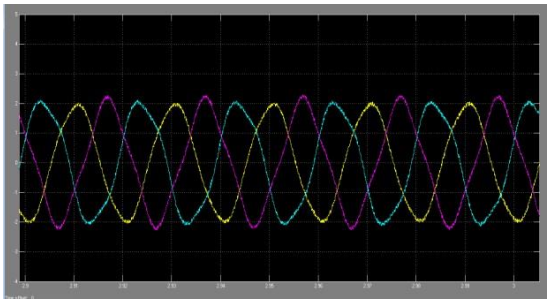

b. Ilabc

Fig.13.Primaryandsecondarycurrentwaveformwith harmonics spectrum analysis of bothcurrentswhileshunt converterdisabled.

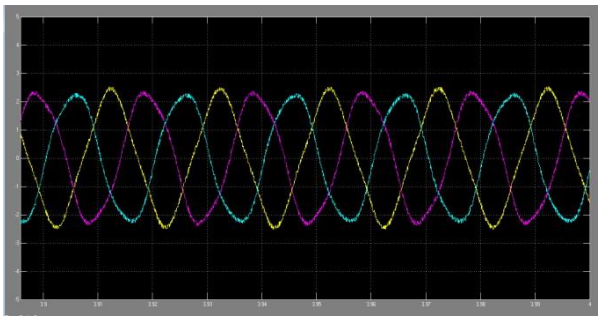

a. Ipabc

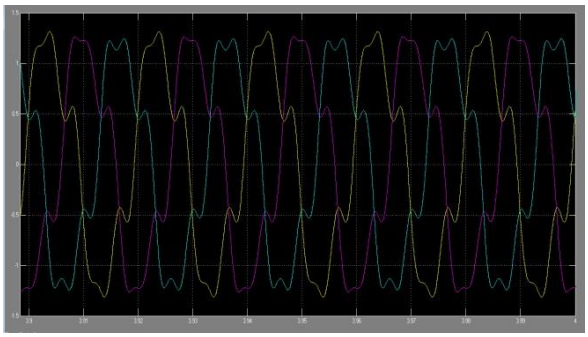

b. Ilabc

Fig. 14. Primary and secondary current waveformwithharmonicsspectrumanalysisofbothcurrentswhile shuntconverter enabled.

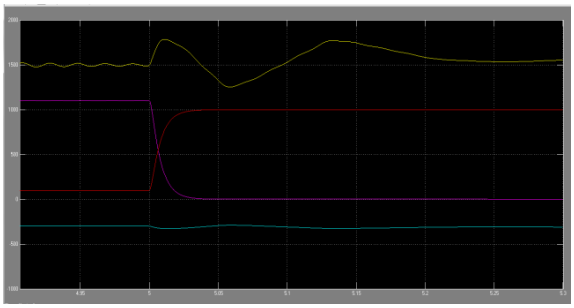

Fig. 15. Active and reactive power through theprimaryandshuntwindingwithenabledReactive PowerController.

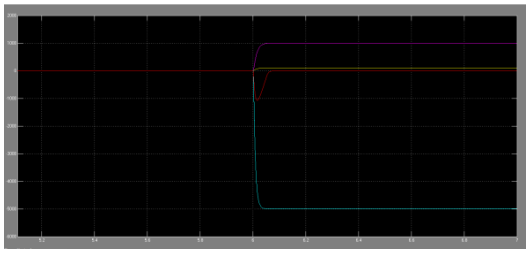

Fig. 16. Active and reactive power through thesecondary and series winding during activation oftheSecondaryCurrent Controller.

ISSN: 1832-5505
Vol-9 Issue-04 Oct 2021

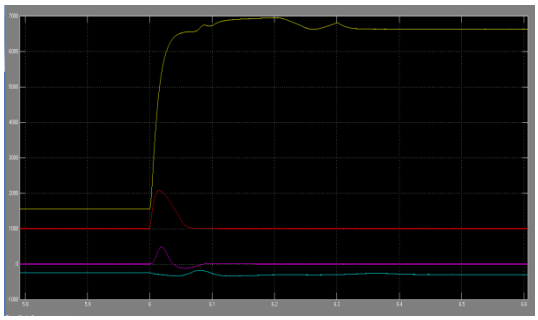

Fig.17 Active and reactive power through theprimaryandshuntwindingsduringstepchangein referenceoutput power

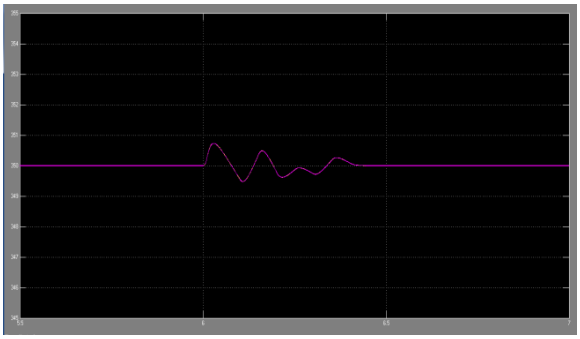

Fig.18DCbusvoltageduringchangeinreferenceoutputpower.

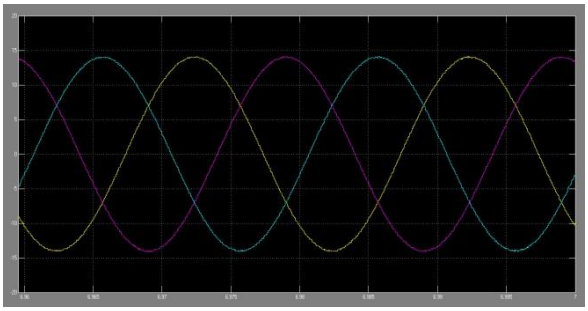

a. Ipabc

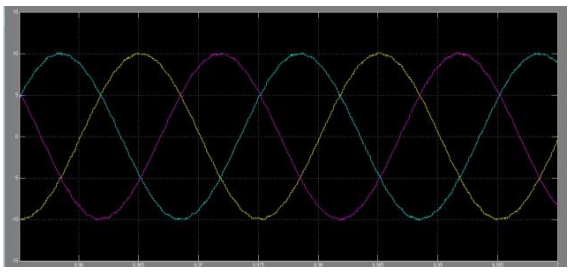

b. Ilabc

Fig. 19. Primary and secondary current waveformand harmonics spectrum with all controllersenabled.

b. Simulationresultsusingfuzzylogiccontroller

With the use of the displaying method discussed in Section II, the CPAT plan in Figure 4 was shown with respect to the cutoff points in Table I. The model of the transformer takes into account the following parameters: member region A, number of turns N, limit length lL, and bother length lY. As shown in Figure 8, the standard firm structure was linked to the discretionary and crucial windings. Since both the basic and the assistant are activated by a voltage that is almost similar in this state, there is no force stream between them. After all is said and done, the two windings would be used to activate the CPAT's polarising current. During this time, the shunt and strategy converters combined zero current and voltage since the shunt and strategy controllers were both wounded. As seen in Figure 20, the primary current mostly consisted of the third, fifth, and seventh request noises. Central CPAT charging current and DC transport guideline current made up the majority of the essential current in this case since there was no force stream connecting the essential and auxiliary currents. The critical current waveform was severed from these segments by the shunt music controller adjusted to these frequencies, as shown in Figure 21. Since these symphonious flows would not be amplified, uncompensated higher-request noises were not a concern. The fundamental current would extend beyond the polarising current but remain under the gauges. As shown in Figure 22, the shunt open power controller was activated with a reference of 0 VAR, causing the shunt converter to provide the responsive power needed by the CPAT.

Figure 23 shows that the assistant current controller was turned on with a reference power stream of 0 kVAR between the basic and discretionary sources and a 5 kW reference power. The action converter provided the strategy twisting with the responsive capacity to alter the common impedance between the main and secondary windings. At that same instant, the fundamental power also altered since the helper had infused the system with ability, which the basic had obtained (Fig.24). As seen in Figure 25, the DC transport controller maintained a constant DC transport voltage throughout the movement. Figure 26 shows the resulting basic and discretionary current waveforms from this reference. From start to finish, the graph displays how well the music controller contracted the basic current music at the tuned frequencies.

ISSN: 1832-5505
Vol-9 Issue-04 Oct 2021

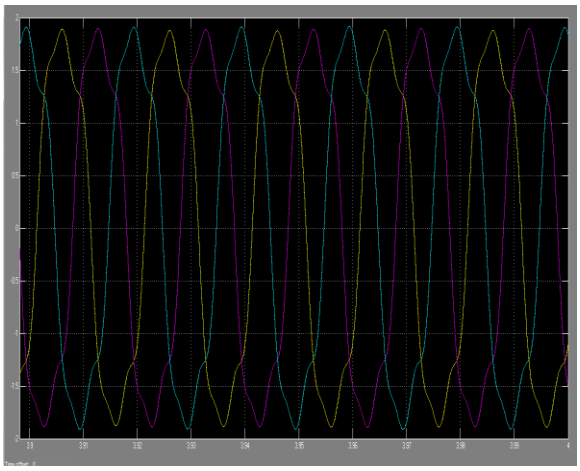

a. Ipabc

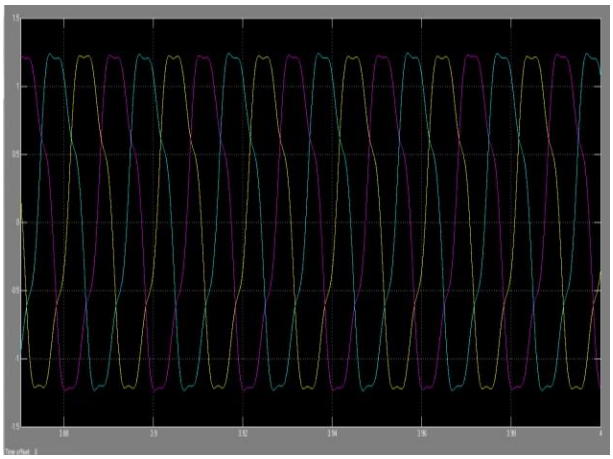

b. Ilabc

Fig.20.Primaryandsecondarycurrentwaveformwith harmonics spectrum analysis of bothcurrentswhileshunt converterdisabled.

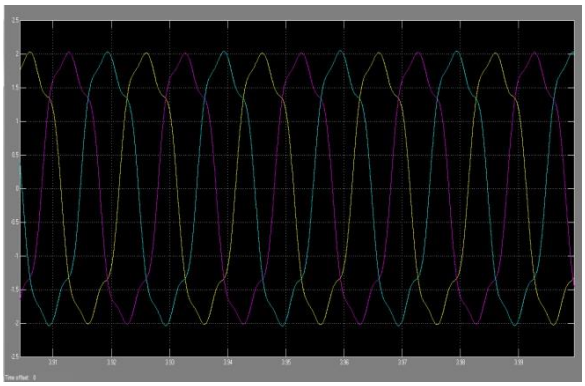

a. Ipabc

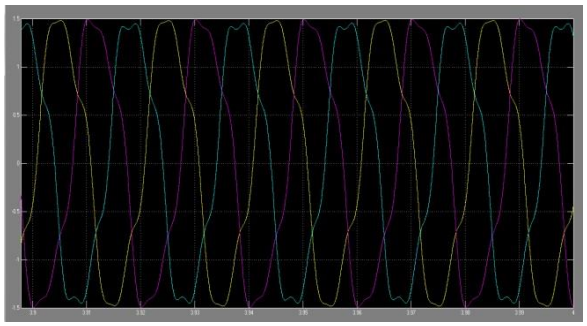

b. Ilabc

Fig. 21. Primary and secondary current waveformwithharmonicsspectrum analysisofbothcurrentswhile shuntconverter enabled.

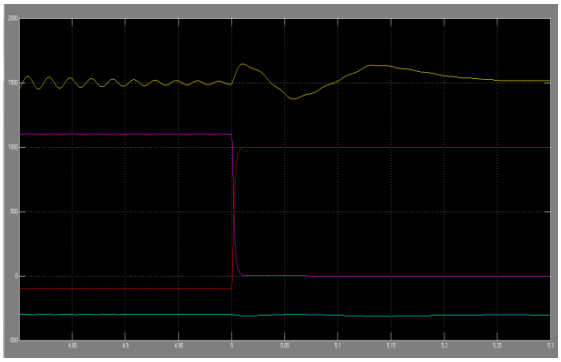

Fig. 22. Active and reactive power through theprimaryandshuntwindingwithenabledReactive PowerController.

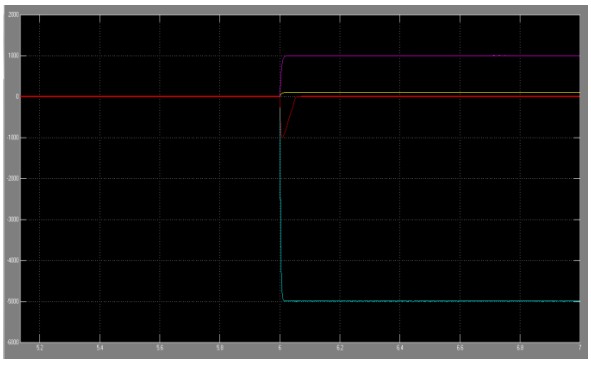

Fig. 23. Active and reactive power through thesecondaryandserieswindingduringactivationof theSecondaryCurrent Controller.

ISSN: 1832-5505
Vol-9 Issue-04 Oct 2021

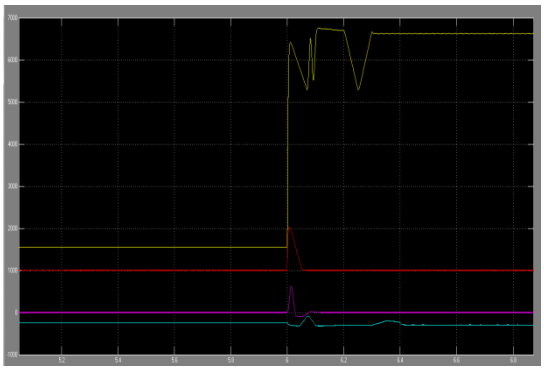

Fig 24 Active and reactive power through theprimaryandshuntwindingsduringstepchangein referenceoutput power

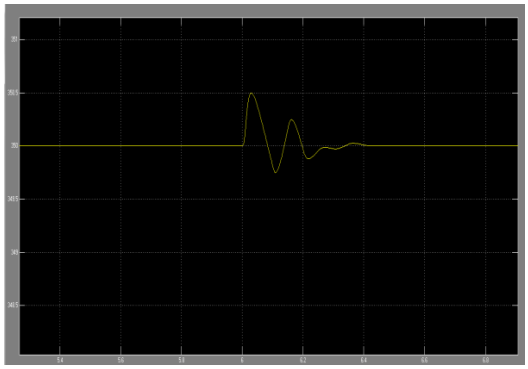

Fig25DCbusvoltageduringchangeinreferenceoutputpower.

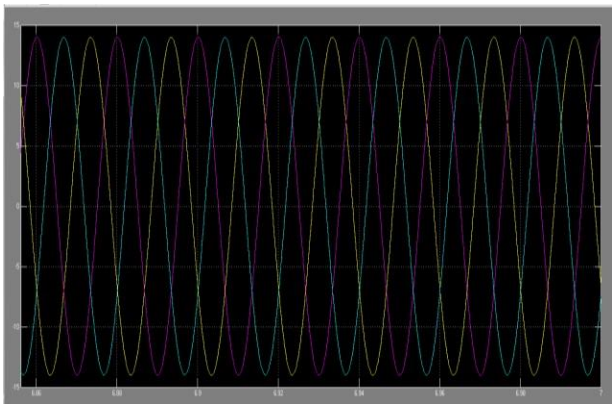

a. Ipabc

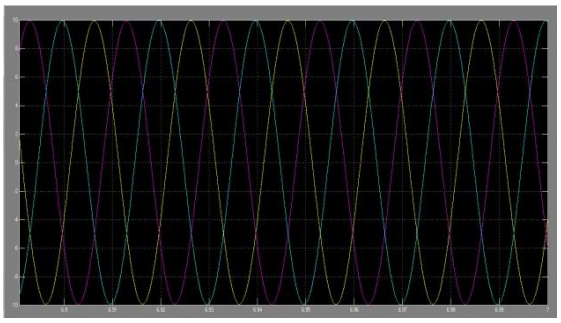

b. Ilabc

Fig. 26. Primary and secondary current waveformand harmonics spectrum with all controllersenabled.

V. CONCLUSION

The CPAT-UPFC, described in this work, is a trio of single-stage CPATs that have been equipped with a sequential converter and a fuzzy logic controller. A CPAT's accessible shunt and arrangement windings allow for the provision of various network administrations, such as responsive force pay, force stream management, and lattice consonant flows termination. A 5-transport power framework model and toughened lattice activity were used to develop and study non-direct and straight CPAT display methodologies. An exploratory model demonstrating a CPAT's ability to function as a UPFC and reenactments have been used to evaluate the presented control architecture. The findings of the inquiry, recreation, and trial confirm that the CPAT-UPFC can provide the required kinds of support.

VI. REFERENCES

1) M.S.Mahmoud,M.SaifUrRahmanandF. M.A.L.Sunni,“Reviewofmicrogridarchitectu ressystemofsystemsperspective,”IETRenewa blePowerGeneration,vol.9,no.8,pp.1064-1078,Nov. 2015.
2) Q.Huang,S.Jing,J.Li,D.Cai,J.Wuand W. Zhen, “Smart Substation: State of the ArtandFutureDevelopment,”IEEETrans.Pow er Del., vol. 32, no. 2, pp. 1098-1105,Apr.2017.
3) H. Liao and J. V. Milanović, “On capabilityofdifferentFACTSdevicestomitigat earangeofpowerqualityphenomena,”IETGen eration,Transmission&Distribution,vol.11, no. 5,pp.1202-1211,Mar.2017.
4) M.Shahparasti,M.Mohamadian,P.T.Babolia ndA.Yazdianp,“TowardPowerQualityManag ementinHybridAC–DC

ISSN: 1832-5505
Vol-9 Issue-04 Oct 2021

Microgrid Using LTC-L Utility InteractiveInverter:LoadVoltage–GridCurrentTradeoff," IEEE Trans. Smart Grid, vol. 8,no.2, pp.857-867, Mar. 2017.

5) J.BarrandR.Majumder,"IntegrationofDistributedGenerationintheVolt/VARManagement System for Active DistributionNetworks," IEEE Trans. Smart Grid, vol. 6,no.2, pp.576-586, Mar. 2015.
6) M. A. Sayed and T. Takeshita, "All NodesVoltageRegulationandLineLossMinimization in Loop Distribution SystemsUsing UPFC," IEEE Trans. Power Electron.,vol.26, no. 6,pp.1694-1703,June 2011.
7) F.Z.Peng,"FlexibleACTransmissionSystems (FACTS)andResilientACDistributionSystems(RACDS)inSmartGrid,"Proc.IEEE,vol.105, no.11,pp.2099-2115,Nov. 2017.
8) E.Rakhshani,D.Remon,A.M.Cantarellas, J.M.GarciaandP.Rodriguez,"VirtualSynchronousPowerStrategyforMultipleHVDC Interconnections of Multi-Area AGCPower Systems," IEEE Trans. Power Syst.,vol. 32, no. 3,pp.1665-1677,May2017.
9) W.Litzenberger,K.MitschandM.Bhuiyan,"WhenIt'sTimetoUpgrade:HVdcandFACTSRenovationintheWesternPowerSystem,"IEEEPowerEnergy Mag., vol. 14, no. 2, pp. 32-41, Mar.2016.
10) M.Andresen,K.Ma,G.DeCarne,G.Buticchi,F.BlaabjergandM.Liserre,"ThermalStressAnalysisofMedium-VoltageConvertersforSmartTransformers,"IEEETrans.PowerElectron., vol. 32, no. 6, pp. 4753-4765, Jun.2017.
11) S.Yang,Y.Liu,X.Wang,D.Gunasekaran, U. Karki and F. Z. Peng, "Modulation andControlofTransformerlessUPFC,"IEEETrans. Power Electron., vol. 31, no. 2, pp.1050-1063,Feb.2016.
12) C.Liangetal.,"HarmonicEliminationUsingParallelDelta-ConnectedFilteringWindingsforConverterTransformersinHVDC Systems," IEEE Trans. Power Del.,vol.32,no.2,pp.933-941,Apr.2017.